Available online at www.sciencedirect.com
ScienceDirect
Journal of Nuclear Materials 360 (2007) 25–31
journal of nuclear materials
www.elsevier.com/locate/jnucmat

# Electrochemical behaviour of gadolinium ion in molten LiCl–KCl eutectic

C. Caravaca *, G. de Córdoba, M.J. Tomás, M. Rosado

*CIEMAT/Nuclear Fission Division/Radioactive Wastes Unit, Avda, Complutense, 22, Madrid 28040, Spain*

---

## Abstract

This work presents the electrochemical study of $GdCl_3$ in the molten LiCl–KCl eutectic in the temperature range 723–823 K. Transient electrochemical techniques such as cyclic voltammetry and chronopotentiometry, on an inert metallic tungsten working electrode, have been used in order to investigate the reduction mechanism and transport parameters. This study shows that $Gd^{3+}$ ions are reduced to Gd metal by a single step mechanism with exchange of three electrons. Diffusion coefficient of $GdCl_3$ ions was determined at various temperatures, at 723 K the value is $D = 0.88\ 10^{-5}\ cm^2\ s^{-1}$. Apparent standard reduction potential of the redox couple $Gd^{3+}/Gd$ has been determined by the open-circuit chronopotentiometry technique at several temperatures. Also the Gibbs free energy of $GdCl_3$ formation was determined and compared with thermodynamic data for pure compounds in the supercooled state in order to estimate the activity coefficient of $Gd^{3+}$ in the molten LiCl–KCl eutectic.

---

## 1. Introduction

Partitioning and transmutation (P&T) concepts are considered as an efficient way to reduce the long-term radiotoxicity of nuclear waste by recycling the actinides. For these concepts it is essential the efficient recovery and multi-recycle of actinides. In the application of the P&T strategies the actinides are recycled and burned in dedicated reactors. Fuels proposed will contain a significant quantity of Pu and minor actinides (MA)(Np, Am, Cm), possibly in inert matrices (U free), and will reach high burn-ups. Pyrochemical separation techniques offer advantages compared to hydrometallurgical separation processes, mainly due to the high radiation stability of the salt solvent and the resulting shorter cooling times [1].

Electrochemical methods such as electrolysis or electrorefining as well as reductive extraction are used in different pyrochemical partitioning processes. The application to the reprocessing of metallic fuel from the EBR-II reactor is the best known process [2]. In this process the actinides are separated from the bulk of fission products by electrotransport in a molten salt electrolyte, the U is electrodeposited into a solid cathode and the Pu and MA into a liquid Cd cathode [3]. Additional systems for the separation of Pu and MA are now being developed such as reductive extraction in a molten metal/molten salt system [4–6], or the

---

* Corresponding author. Tel.: +34 91 3466216; fax: +34 91 3466233.
*E-mail address:* c.caravaca@ciemat.es (C. Caravaca).

0022-3115/$ - see front matter © 2006 Elsevier B.V. All rights reserved.
doi:10.1016/j.jnucmat.2006.08.009

electrotransport into different molten metal cathodes such as Bi [7], or more recently solid Al [8].

The aim of these investigations is to optimize the separation efficiency of MA and to minimize the content of fission products, especially the rare earth elements due to the similar chemical properties and its neutronic poison effect. For this purpose, it is important to know accurately the electrochemical and thermodynamic properties of actinides and rare earths elements in each phase. Electrochemical data for actinides [9–14] and lanthanides [15–18] obtained using different electrochemical techniques in LiCl–KCl are available, and from these data thermodynamic quantities were derived (enthalpy and entropy of formation, activity coefficients). However, in some cases some discrepancies were observed. To try to solve this, our group has performed a systematic electrochemical study of some actinides [19,20] and rare earths [18,21] in the molten LiCl–KCl eutectic in order to investigate mechanisms of reduction, diffusion coefficients and thermodynamic properties.

The investigation presented in this paper is part of the work carried out within the EUROPART Project of the EU, and presents the main results obtained in the electrochemical study of the LiCl–KCl–$GdCl_3$ system.

## 2. Experimental

### 2.1. Chemicals and apparatus

Electrochemical experiments were carried out in a quartz sealed cell under pure Ar atmosphere (Air liquide, $H_2O < 0.5$ ppm and $O_2 < 0.1$ ppm). The electrodes and the Chromel–Alumel thermocouple (in a $Al_2O_3$ tube sheath) were positioned in the electrochemical cell, that supported a vitreous carbon crucible containing the salt mixture.

The electrolytic bath consisting of $Gd^{3+}$ dissolved in LiCl–KCl eutectic (Merck 99.5%) was prepared from anhydrous $GdCl_3$ (Aldrich 99.99%). The eutectic melt was kept for 8–10 h at 200 °C, afterwards, the temperature was raised up to 450 °C until melt. Then, the solvent was purified bubbling HCl (g), and then Ar in order to remove the HCl dissolved into the molten salt [22,23].

Transient electrochemical techniques used, i.e. cyclic voltammetry and chronopotentiometry were carried out in an electrochemical cell having a three-electrode set-up. The measurements were carried out using an Autolab PGSTAT30 potentiostat (Eco-Chimie) with a specific GPES electrochemical software version 4.9. For the semi-integral analysis of the cyclic voltammograms the GPES software was also used.

Inert working electrode was prepared using 1 mm metallic W wire and immersed into the molten bath between 3 and 10 mm. The surface area was determined after each experiment by measuring the immersion depth of the electrode. Counter electrode was prepared either using a 1 mm Mo wire coiled or a 3 mm vitreous carbon rod. The reference electrode was an Ag/AgCl–LiCl–KCl (0.75 mol $kg^{-1}$) prepared in a Pyrex glass tube.

Samples (of about 200 mg) were taken from the molten salt, dissolved and diluted in nitric acid. The gadolinium concentration was determined by ICP-MS analysis.

## 3. Results and discussion

### 3.1. Cyclic voltammetry

Cyclic voltammetry was carried out on a tungsten electrode in a LiCl–KCl–$GdCl_3$ melt at several temperatures (723–873 K). The cathodic and anodic limits of the electrochemical window corresponds to the reduction of $Li^+$ and the oxidation of chloride ions, respectively.

The cyclic voltammogram of Fig. 1 shows a single cathodic peak $I_C$ at $\approx -2.23$ V versus the Ag/AgCl reference electrode. The sharp anodic peak (at $-2.04$ V) is typical of the dissolution of a metal deposited in the cathodic sweep, stripping peak. According to this, we can assume that

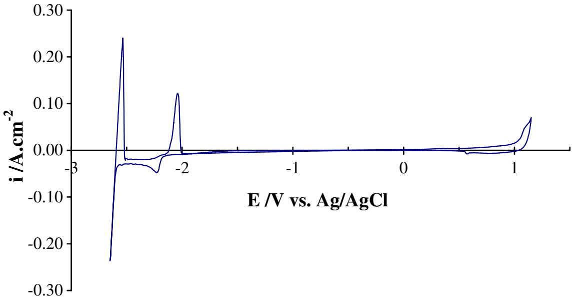

Fig. 1. Cyclic voltammogram of LiCl–KCl–$GdCl_3$ ($2.03 \times 10^{-2}$ mol/kg) at 723 K. Working electrode: W (surface area = 0.352 $cm^2$); counter electrode: vitreous carbon, reference electrode: Ag/AgCl (0.75 mol $kg^{-1}$ in LiCl–KCl); scan rate = 0.2 V $s^{-1}$.

gadolinium metal is deposited in a single step by reduction of Gd(III) ions into Gd(0). The height of the peak at −2.23 V, that corresponds to the electrochemical reduction of gadolinium (III) ions, increases with the Gd concentration increase. A linear relationship between the current density of the cathodic peak and the ion concentration was observed.

At more anodic potentials (at about −1.5 V) a wave with a low current density is observed; it is attributed to impurities in the solvent melt, since its intensity does not depend on the Gd ion concentration. This has been corroborated by the study performed to the solvent by chronopotentiometry at zero current.

The current of the cathodic peak is directly proportional to the square root of the polarization rate ($v$) as can be observed in Fig. 2. Besides, up to scan rates of 100 mV s$^{-1}$ the value of peak potential, $E_p$, is constant and independent of the sweep potential rate. According to the theory of linear sweep voltammetry [24], the electrode process is reversible and controlled by the rate of the mass transfer. For higher sweep rates, higher than 100 mV s$^{-1}$, the cathodic peak is shifted towards more cathodic values, indicating that the system becomes quasi-reversible [25].

The number of exchanged electrons in the electroreduction process was determined by means of the square wave voltammetry technique [26,27], measuring the width of the half peak ($W_{1/2}$ in volts). Eq. (1) was applied in the region in which the current peak is proportional to the square root of the frequency of the potential signal, that is, at low frequency values [10,28]. The number of exchanged electrons obtained from this analysis was close to 3

$$W_{1/2} = 3.52\frac{RT}{nF}. \tag{1}$$

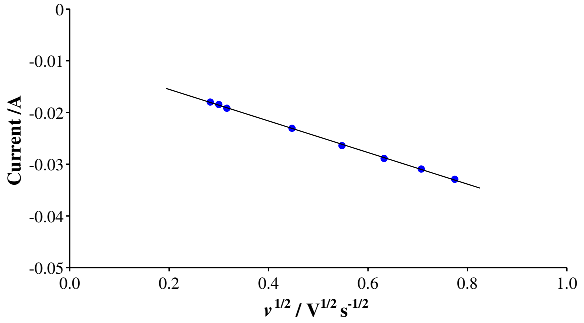

Fig. 2. Dependence of peak currents of the electroreduction reaction of $Gd^{3+}$ on the sweep potential rate. $[Gd^{3+}] = 1.19 \times 10^{-4}$ mol cm$^{-3}$, $T = 723$ K, working electrode: W ($S = 0.28$ cm$^2$), counter electrode: Mo.

### 3.2. Diffusion coefficient

Diffusion coefficient of $GdCl_3$ in molten LiCl–KCl was determined using three different techniques, cyclic voltammetry (CV), convolution and chronopotentiometry (CP).

For cyclic voltammetry, the diffusion coefficient of $GdCl_3$ ions was estimated using Eq. (2) for reversible soluble–insoluble systems [29]:

$$I_p = -0.6105SC\frac{(nF)^{3/2}}{(RT)^{1/2}}D^{1/2}v^{1/2}, \tag{2}$$

where $S$ is the electrode surface area in cm$^2$, $C$ is the solute concentration in mol cm$^{-3}$, $D$ is the diffusion coefficient in cm$^2$ s$^{-1}$, $F$ is the Faraday's constant, 96493$C$, $R$ is the universal gas constant, $n$ is the number of exchanged electrons, $v$ is the potential sweep rate in V s$^{-1}$ and $T$ is the absolute temperature in K.

However, we do not consider these values as very accurate since as it has been previously indicated, the Gd(III)/Gd(0) system is quasi-reversible, and we have observed that the values obtained using this technique, that are indicated in Table 1, differs significantly with those obtained by the other electrochemical techniques. This discrepancy that is attributed to the non reversibility of the system, has also been observed by Martínez [30]. Therefore, we consider that the use of this equation is not appropriated for all potential scan rates in the Gd(III)/Gd(0) system, despite several authors consider that this equation can be applied in these conditions.

The linear potential sweep data were transformed according to the convolution principle [28,31,32] into a curve that resembles a steady-state voltammetric curve. This technique is more reliable since it uses the whole curve instead of only the peaks [28].

According to the theory of convolution, the diffusion coefficient can be calculated using Eq. (3), that is reliable for reversible and non-reversible systems [33]:

$$m^* = -nFSCD^{1/2}, \tag{3}$$

being $m^*$, the limiting current of the convoluted curve of the corresponding cyclic voltammogram. Diffusion coefficient values are indicated in Table 1 for all the temperatures tested.

Fig. 3 shows the evolution of the chronopotentiograms of $GdCl_3$ with the applied current intensity at

Table 1
Diffusion coefficients of $GdCl_3$ in LiCl–KCl at several temperatures

| $T$ /K | $D \times 10^5$ /cm$^2$ s$^{-1}$ | | | | |
|---|---|---|---|---|---|
| | (CV) | (Convolution) | (CP) | Lantelme [38] | Iizuka [40] |
| 723 | 0.31 | 0.88 | 0.64 | 0.74 | 1.00 |
| 773 | 0.53 | 1.15 | 1.18 | 1.05 | 1.41 |
| 822 | 1.09 | 1.65 | 1.83 | 1.44 | 1.91 |
| 873 | 1.28 | 2.22 | – | 1.90 | 2.49 |
| $E_A$ /kJ mol$^{-1}$ | −53.38 | −32.45 | −52.14 | −33.03 | −31.93 |

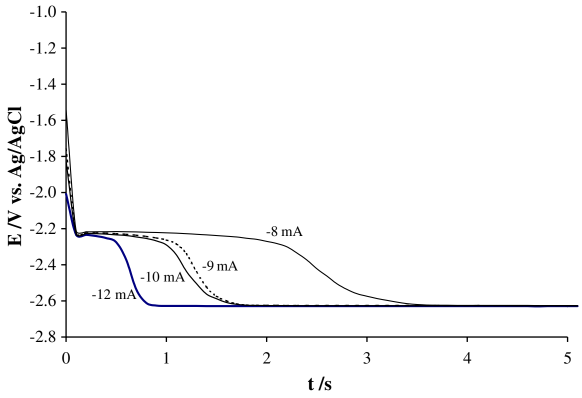

Fig. 3. Linear relationship of the neperian logarithm of the diffusion coefficient of Gd(III) as a function of the reverse of the absolute temperature. Temperature range 723–873 K.

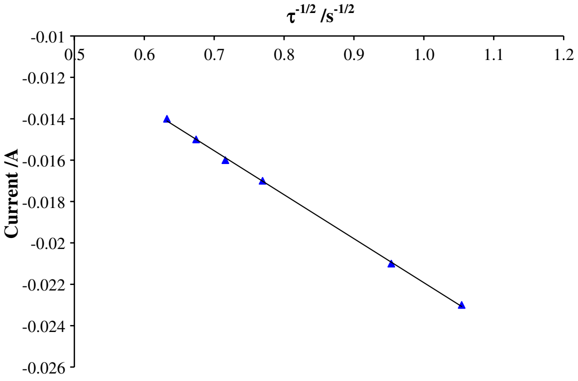

Fig. 4. Chronopotentiogramas of $GdCl_3$ in LiCl–KCl eutectic. $GdCl_3$ concentration $1.19 \times 10^{-4}$ mol cm$^{-3}$, $T = 723$ K, working electrode: W ($S = 0.286$ cm$^2$), counter electrode: Mo.

a tungsten working electrode. The curves exhibits a single wave associated to the reduction of gadolinium ions into metal in the same potential range at those observed in the cyclic voltammograms.

The transition time, $\tau$, was obtained by measuring the duration of the first part of the chronopotentiogram according to the methodology indicated in Refs. [34–36]. Several current intensities were applied, and the plot of $I$ versus $\tau^{-1/2}$ gives a straight line as shown in Fig. 4. In addition, the chronopotentiometric curves did not shift in the direction of negative potentials with increasing the current density. Based on these results, the electrochemical reduction of Gd(III) ions can be considered a diffusion controlled process [37], and the diffusion coefficient of Gd(III) in the LiCl–KCl can be calculated using the Sand equation [28]:

$$I\sqrt{\tau} = \frac{nFCS\sqrt{\pi D}}{2} = \text{constant}. \tag{4}$$

Table 1 shows the diffusion coefficient of $Gd^{3+}$ in LiCl–KCl at several temperatures obtained by the technique of CP along with those obtained by other techniques. Results are in fair agreement with each other, taken into account that the calculations are affected by experimental uncertainties such as determination of the active electrode surface area and by the graphical evaluation of the transition times in the chronopotentiograms.

In Table 1, the results obtained in the present work are also compared with values obtained from the literature. It is observed that values obtained by the convolution technique are in good agreement with those of Lantelme et al. [38,39] and Iizuka [40]. The results from chronopotentiometry are also in fair agreement except at 723 K, and those obtained from cyclic voltammetry differs significantly, as mentioned previously.

The influence of the temperature on the value of $D$ was determined plotting the $\ln D$ versus the reverse of absolute temperature, as it is shown in Fig. 5. The results obey the Arrhenius's law expressed as [28]

$$D = D_0 \exp\left(-\frac{E_A}{RT}\right), \tag{5}$$

where $E_A$, the activation energy for the diffusion, is found from data of Fig. 5 to be equal to

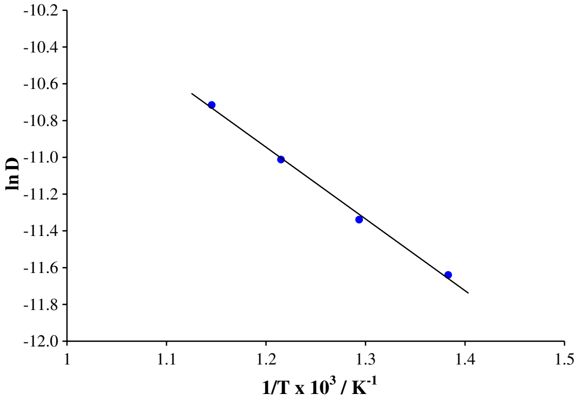

Fig. 5. Dependence of current versus $\tau^{-1/2}$. $GdCl_3$ concentration: $5.04 \times 10^{-5}$ mol cm$^{-3}$, $T = 723$ K, working electrode: W ($S = 0.286$ cm$^2$), counter electrode: Mo.

$-32.45$ kJ mol$^{-1}$, and the pre-exponential term $D_0$ is: $1.99 \times 10^{-3}$ cm$^2$ s$^{-1}$. The values of activation energy obtained by the different techniques and those found in the bibliography are indicated in Table 1. It is observed a good agreement for the value obtained by convolution technique with those previously published by several authors, while those obtained by cyclic voltammetry or chronopotentiometry are quite higher.

### 3.3. Apparent standard potential

The apparent standard potential of the redox couple Gd(III)/Gd(0) was determined at several temperatures. For the measurement, the technique of open-circuit chronopotentiometry of a solution containing a $GdCl_3$ concentration in LiCl–KCl of $1.66 \times 10^{-3}$ mole fraction was used. A short cathodic polarisation was applied, 1 min, in order to form in situ a metallic deposit of Gd on the W electrode, and then the open-circuit potential of the electrode was measured versus time. The pseudo-equilibrium potential of the redox couple $Gd^{3+}/Gd$ was measured and the apparent standard potential, $E^{*\circ}$, was determined using the Nernst equation:

$$E = E^{*\circ}_{\mathrm{Gd(III)/Gd(0)}} + \frac{RT}{nF} \ln X_{\mathrm{GdCl_3}}, \qquad (6)$$

being,

$$E^{*\circ} = E^{\circ}_{\mathrm{Gd(III)/Gd(0)}} + \frac{RT}{nF} \ln \gamma_{\mathrm{GdCl_3}}. \qquad (7)$$

The apparent standard potential is obtained in the mole fraction scale versus the Ag/AgCl (0.75 mol kg$^{-1}$) reference electrode and then transformed into values of potential versus the $Cl_2/Cl^-$ reference electrode scale. To carry out this conversion, it is assumed that the activity coefficients of Ag and AgCl are the unity [14]. Thus, the potential of the reference electrode can be defined as

$$E_{\mathrm{AgCl}} = E^{\circ}_{\mathrm{AgCl}} + \frac{RT}{nF} \ln[\mathrm{AgCl}]. \qquad (8)$$

For a concentration of AgCl equal to 0.75 mol kg$^{-1}$, the value of $E^{\circ}_{\mathrm{AgCl}}$ relative to the $Cl_2/Cl^-$ reference electrode is given by the following expression according to Mottot [15]:

$$E^{\circ}_{\mathrm{AgCl}} = -1.224 + 2.92 \times 10^{-4} \times T\ (\mathrm{K}). \qquad (9)$$

At 723 K, Eq. (8) yields the potential of the reference electrode $E_{\mathrm{AgCl}} = -1.050$ V vs. $Cl_2/Cl^-$.

The apparent standard potential value obtained a 723 K is $E^{*\circ}_{\mathrm{Gd(III)/Gd(0)}} = -3.0397$ V. This value is in good agreement with the values obtained by Lantelme et al. $-3.0354$ V [38] and $-3.0411$ V [39], Roy et al. $-3.044$ V [17] and Yang and Hudson $-3.0477$ V [41], and slightly lower than that of Fusselman et al. $-3.056$ V [14].

The experimental data obtained in this work in the temperature range of 723–873 K are plotted in Fig. 6 in which are also plotted the values of standard potential obtained by other authors.

### 3.4. Thermodynamic properties

The apparent standard Gibbs energy of formation $\Delta G^{*}_{\mathrm{GdCl_3}}$ is calculated according to

$$\Delta G^{*}_{\mathrm{GdCl_3}} = nFE^{*\circ}_{\mathrm{Gd(III)/Gd}}. \qquad (10)$$

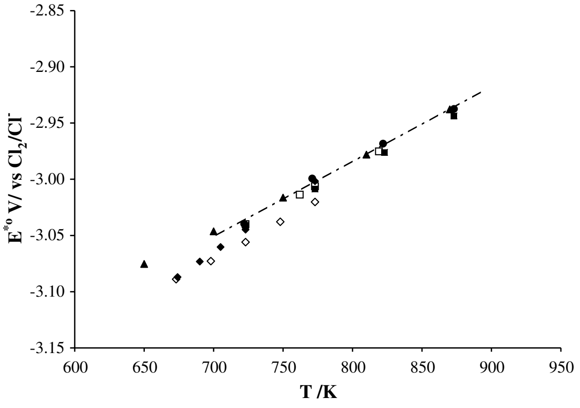

Fig. 6. The apparent standard potential of the Gd(III)/Gd(0) redox couple in LiCl–KCl; ●, present work, ▲, Lantelme et al. [38], ■, Lanteleme et al. [39], ◇, Fusselman et al. [14], □ Roy et al. [17] and ◆ Yang and Hudson [41].

Table 2
Variation of the activity coefficients of $GdCl_3$ in LiCl–KCl eutectic as a function of the temperature

| $T$ /K | $10^3\gamma$ /f-MPD | $10^4\gamma$ /HSC 4.0 |
|---|---|---|
| 722 | 2.59 | 0.592 |
| 771 | 4.60 | 1.50 |
| 822 | 4.87 | 2.21 |
| 873 | 5.11 | 3.09 |

The plot of the $\Delta G^*_{GdCl_3}$ as a function of the temperature shows a linear dependence. The least square fit of the standard Gibbs energy versus the temperature can be expressed by the following equation:

$$\Delta G^*_{GdCl_3} = \Delta H^*_{GdCl_3} - T\Delta S^*_{GdCl_3}, \tag{11}$$

from which, values of enthalpy and entropy of formation can be obtained:

$$\Delta G^*_{GdCl_3} = 1019 + 0.194T/\ \mathrm{kJ\,mol^{-1}}. \tag{12}$$

This equation is in good agreement with that obtained by Lantelme et al.: $1003.19 + 0.242\,T$ ($\mathrm{kJ\,mol^{-1}}$) [38] and Fusselman et al.: $1028.9 + 0.200T$ ($\mathrm{kJ\,mol^{-1}}$) [14], using emf measurements.

The activity coefficient of $GdCl_3$ in the LiCl–KCl eutectic, was determined from the difference between the Gibbs energy of formation derived from the electrochemical measurements and the Gibbs energy of formation for pure compounds in the supercooled state [42], according to the equation:

$$2.3RT\log\gamma_{GdCl_3} = \Delta G^*_{GdCl_3} - \Delta G^\circ{}_{GdCl_3(sc)} \tag{13}$$

The activity coefficient values derived using this reference state are given in Table 2. In order to compare these data to those obtained using different reference states for pure compounds, in Table 2 are also given values obtained considering the state of pure compounds in liquid state [43]. It can be seen that the activity coefficients differ significantly depending on the thermodynamic data base used.

## 4. Conclusions

The electrochemical behaviour of $GdCl_3$ in molten LiCl–KCl eutectic has been investigated. It has been shown that Gd(III) is reduced to Gd metal by a single step mechanism and that the diffusion coefficient of $Gd^{3+}$ ion is about $0.88 \times 10^{-5}\ \mathrm{cm^2\,s^{-1}}$ at 723 K. The apparent standard potential and the Gibbs energy of formation of $GdCl_3$ have been measured using the chronopotentiometry at open-circuit technique and are in good agreement with results found in the literature, using emf measurements. The activity coefficient of $GdCl_3$ in the molten LiCl–KCl eutectic was calculated to be $\gamma_{GdCl_3} = 2.59 \times 10^{-3}$. However, it is observed that these values can change significantly depending on the source taken for the Gibbs energy of formation as reference system.

## Acknowledgement

The authors wish to thank J. Quiñones and J.M. Cobo for the help with the ICP-MS analysis, and V. Smolenski for the technical discussions.

## References

[1] OCDE/NEA Report. Accelerator-driven systems (ADS) and fast reactors (FR) in advanced nuclear fuel cycles. A comparative study, 2002, p. 1.
[2] J.J. Laidler, J.E. Battles, W.E. Millar, J.P. Ackerman, E.L. Carls, Prog. Nucl. Energy 31 (1997) 131.
[3] T. Nishimura, T. Koyama, M. Iizuka, H. Tanaka, Prog. Nucl. Energy 33 (3/4) (1998) 381.
[4] K. Kinoshita, T. Inoue, S.P. Fusselman, D.L. Grimmett, J.J. Roy, R.L. Gay, C.L. Krueger, C.R. Nabelek, T.S. Strovick, J. Nucl. Sci. Technol. 36 (1999) 189.
[5] M. Kurata, Y. Sakamura, T. Inoue, in: Proceedings third Information Exchange Meeting on Actinide and Fission Products Partitioning and Transmutation, Cadarache, France, December 1994, 407.
[6] O. Conocar, N. Douyere, J. Lacquement, J. Alloys Compd. 389 (2005) 29.
[7] O. Shirai, K. Uozumi, I. Iwai, Y. Arai, J. Appl. Electrochem. 34 (2004) 323.
[8] J. Serp, M. Allibert, A.L. Terrier, R. Malmbeck, M. Ougier, J. Rebizant, J.-P. Glatz, J. Electrochem. Soc. 152 (2005) C167.
[9] L. Martinot, Molten salt chemistry of actinides, North Holland, 1991, p. 241.
[10] K. Serrano, PhD thesis, Univertisé Paul Sabatier, 1998.
[11] J. Serp, R.J.M. Konings, R. Malmbeck, J. Rebizant, C. Scheppler, J.-P. Glatz, J. Electroanal. Chem. 561 (2004) 143.
[12] D. Lambertin, PhD thesis, Université Pierre et Marie Curie, Paris VI, 2001.
[13] C. Pernel, PhD thesis, Insitute National Polytechnique de Grenoble, 2002.
[14] S.P. Fusselman, J.J. Roy, D.L. Grimmett, L.F. Grantham, C.L. Krueger, C.R. Nabelek, T.S. Storvick, T. Inoue, T. Hijikata, K. Kinoshita, Y. Sakamura, K. Uozumi, T. Kawai, J. Takahashi, J. Electrochem. Soc. 146 (1999) 2573.
[15] Y. Mottot, PhD thesis, Université Pierre et Marie Curie, Paris VI, 1986.
[16] M.R. Bermejo, PhD thesis, Universidad de Valladolid, 2003.
[17] J.J. Roy, L.F. Grantham, L.R. McCoy, C.L. Krueger, T.S. Storvic, T. Inoue, H. Miyashiro, N. Takahashi, Mater. Sci. Forum 73–75 (1991) 547.

[18] C. Caravaca, G. Córdoba, Report CIEMAT, DFN/RR-04/IF04, 2004.

[19] C. Caravaca, A. Laplace, J. Vermeulen, J. Lacquement, Report CIEMAT, DFN/RA-05/SP-02, 2002.

[20] G. Córdoba, C. Caravaca, G. Piña, A. Laplace, L. Blarait, J. Lacquement, Report CIEMAT, DFN/RR-03/IF-05, 2005.

[21] G. Córdoba, C. Caravaca, J. Electroanal. Chem. 572 (2004) 145.

[22] H.A. Laitinen, H. Ferguson, R.A. Osteryoung, J. Electrochem. Soc. 104 (1957) 516.

[23] D.G. Lovering, R.J. Gale, Molten Salt Techniques, Vol. 1, Plenum Press, New York, 1983.

[24] M.M. Nicholson, J. Am. Soc. 76 (1954) 2539.

[25] R. Greef, R. Peat, L.M. Peter, D. Pletcher, J. Robinson, Instrumental Methods in Electrochemistry, Ellis Horwood, New York, 1990.

[26] L. Ramaley, M.S. Krause, Anal. Chem. 41 (1969) 1362.

[27] J.G. Osteryoung, R.A. Osteryoung, Anal. Chem. 57 (1985) 101A.

[28] A.J. Bard, L.R. Faulkner, Electrochemical MethodsFundamentals and Applications, John Wiley & Sons, New York, 1980.

[29] T. Store, PhD thesis, Norwegian University of Science and Technology, Electrochemistry Department, 1999.

[30] A.M. Martínez, PhD thesis, Universidad de Valladolid, 1999.

[31] M. Goto, K.B. Oldham, Anal. Chem. 45 (1973) 2043.

[32] J.C. Imbeaux, J.M. Savéant, Electroanal. Chem. Interf. Electrochem. 44 (1973) 169.

[33] M. Greenness, K.B. Oldham, Anal. Chem. 44 (1972) 1121.

[34] B.S. Thalmayer, S. Bruckenstein, D.M. Gruen, J. Inorg. Nucl. Chem. 26 (1964) 347.

[35] R.W. Laity, J.D.E. McIntyre, J. Am. Chem. Soc. 87 (1965) 3806.

[36] P.J. Lingane, D.G. Peters, CRC Crit. Rev. Anal. Chem. (1971) 587.

[37] Z. Galus, Fundamentals of Electrochemical Analysis, Ellis Horwood, London, 1976.

[38] F. Lantelme, Y. Berghoute, J. Electrochem. Soc. 146 (1999) 4137.

[39] F. Lantelme, M. Hamdani, Y. Berghoute, in: Proceedings of EUCHEM 2000, Denmark, 2000, p. 305.

[40] M. Iizuka, J. Elctrochem. Soc. 145 (1998) 84.

[41] L. Yang, R.G. Hudson, Trans. Metall. Soc. AIME 215 (1959) 589.

[42] R.J.M. Konings, The ITU Material Property Data Base for f-elements and Compounds, f-MPD, 2002. Available from: <http//www.f-elements.net.>.

[43] Outokumpu HSC Chemistry 4.0 software.